Review

J. Mex. Chem. Soc. **2025**, *69*(1)
Special Issue

ISSN-e 2594-0317

On the Quest for Understanding Hydrogen Bonding Effects and its Nature

Boris Gutiérrez, Joel Ireta*

Chemistry Department, Universidad Autónoma Metropolinata-Iztapalapa, Av. Ferrocarril San Rafael Atlixco 186, Col. Leyes de Reforma 1 A Sección, Alcaldía Iztapalapa, Mexico City, Mexico.

***Corresponding author:** Joel Ireta, email: iret@xanum.uam.mx

Received May 25th, 2024; Accepted September 23rd, 2024.

DOI: http://dx.doi.org/10.29356/jmcs.v69i1.2296

Abstract. Hydrogen bonding is a prominent non-covalent interaction that influences significatively the properties of the matter in which it is present. In this work it is reviewed some of the contributions of the chemistry department at the Autonomous Metropolitan University-Iztapalapa, to the study of the hydrogen bonding phenomena. Also, it is presented a formula derivation to calculate the hydrogen bond cooperative effect in a linear chain applying the Hellmann-Feynman theorem. In this manner, it is corroborated that the hydrogen bonding cooperative effect in a linear chain arises solely from classical interactions among effective point dipoles.
Keywords: Hydrogen bonding; electronic structure calculations; quantum chemistry.

Resumen. El enlace de hidrógeno es una prominente interacción no covalente que influye significativamente en las propiedades de la materia en la que está presente. En este trabajo se revisan algunos aportes del departamento de química de la Universidad Autónoma Metropolitana-Iztapalapa, al estudio de los puentes de hidrógeno. Además se presenta la derivación de una fórmula para calcular el efecto cooperativo de los puentes de hidrógeno aplicando el teorema de Hellmann-Feynman. De esta manera se corrobora que el efecto cooperativo en la energía de los puentes de hidrógeno surge únicamente de las interacciones clásicas entre dipolos efectivos.
Palabras clave: Puentes de hidrógeno; cálculos de estructura electrónica; química cuántica.

Introduction

The hydrogen bond (hb), an interaction between electron rich and electron poor molecular regions mediated by a hydrogen atom, has been thoroughly investigated both experimental and theoretically since Latimer and Rodebush [1] reported on the presence of such interactions in molecular systems. Usually, the hb is depicted as D-H···A where D stands for donor atom and A for the acceptor atom or region (Fig. 1). The hydrogen bonding phenomenon is so important that it is not an exaggeration to say that life would not be possible without it, e.g., hbs confer peculiar properties to water, proteins, ribonucleic and deoxyribonucleic acids, crucial (bio)molecules for all living systems.

J. Mex. Chem. Soc. **2025**, *69*(1)
Special Issue

ISSN-e 2594-0317

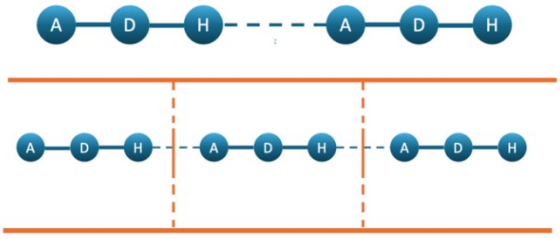

Fig. 1. Top, scheme of a hydrogen bond. The label A stands for acceptor atom or region, D stands for donor atom. Bottom, scheme of an infinite chain of hydrogen bonds modeled as a one-dimensional crystal. Orange lines depict the unit cell. Dashed blue lines indicate the formation of an hb interaction between molecules.

Moreover, hbs exert the forces driving many chemical reactions in solution or in the solid state. Studies about hydrogen bonding can be grossly classified into two kinds, those dealing with the effect of hbs into the physicochemical properties of the systems and those related to advance our understanding of the nature of such interaction. As this work is intended to be part of a special number to celebrate the 50th anniversary of the foundation of the Metropolitan Autonomous University (UAM from the spanish Universidad Autónoma Metropolitana) at Mexico, here it is reviewed some contributions of the chemistry department at UAM, campus Iztapalapa, to the study of the hydrogen bonding phenomena. Particularly, we focus on studies about the proper theoretical description of hbs, their effect on the properties of matter and the hydrogen bonding cooperative effect. Additionally, we discuss about the nature of the hb interaction within the view of the Hellmann-Feynman theorem (HFT). In this manner, we aim for adding further arguments to the ones presented by Nochebuena et al. [2] in one of the reviewed papers, regarding the nature of the hydrogen bonding cooperative effect. In that work [2], it is argued that hydrogen bonding cooperativity results solely from the interaction of classical point dipoles, i.e., not quantum effects are needed to be invoked to understand its origin.

Hydrogen bonding association energy

Interaction energy in hbs range from few, 3 to 4 kcal/mol, to tens, 30 to 40 kcal/mol. From a theoretical standing point, the methods that predict hb association energies within an error of one or two kcal/mol per hb are considered adequate to investigate them. Currently, it is acknowledged that association energies calculated with the coupled cluster method with singles, doubles and perturbative triples (CCSD(T)) excitations are the gold standard [3]. Nevertheless, such method is computationally not feasible to treat systems beyond tens of atoms nowadays. The second order Møller-Plesset perturbation theory (MP2), it is also a reliable level of theory to describe hbs and it can be used to routinely investigate hydrogen bonded systems of tens of atoms. Presently, one may be able to calculate larger systems (of hundreds or even thousands of atoms if large computer facilities are available) using MP2 together with the resolution of the identity approximation [4]. Density functional theory (DFT) in its Kohn-Sham formulation, is also considered adequate to describe hbs but depending on the exchange correlation (xc) functional employed. DFT can be considered the computationally less demanding method to investigate hbs, hence it can be used for investigating more complex (larger) systems than those studied with MP2 or CCSD(T) (Fig. 2).

As mentioned above, DFT accuracy to describe hbs depends on the xc functional employed. For example, following the work of Vargas et al. [5] about the hb strength in formamide and N-methylacetamide dimers, calculated at a MP2 level of theory and extrapolating to the complete basis set limit using the aug-cc-pVXZ basis set family with X = D, T, Q, one of us have shown that DFT with the Perdew-Burke-Ernzerhof (PBE) [6] generalized gradient approximation (gga) to xc describes adequately the hbs [7], as compared to the MP2 results of Vargas et al. However, such description deteriorates as the hb deviates from linearity [7]. To improve the prediction by DFT of the hb strength in situations in which these are nonlinear, we have shown in a later work [8] that empirical corrections to describe dispersion, like that proposed by Tkatchenko and Scheffler

J. Mex. Chem. Soc. **2025**, *69*(1)
Special Issue

ISSN-e 2594-0317

(TS) [9], are required. Yet, one may find systems in which almost any functional fails to properly describe hbs, as in the $(HYN)_2$ hydrogen bonded dimers, with Y = C, Si Ge and Sn [10]. In these dimers, DFT together with almost any gga or hybrid xc functionals predicts a spurious proton transfer event in at least one of the members of the family. We know that the proton transfer event is spurious by comparing the DFT optimized geometries against those obtained with MP2 and reported by us in a previous work [11]. Bautista-Renedo and Ireta have shown that such spurious proton transfer can be remediated fine-tuning the amount of exact exchange in hybrid xc functionals [10]. Still, with these fine-tuned functionals the hb strength is not adequately described in most of the dimers of such family, as compared against CCSD(T) results obtained extrapolating to the basis set limit the aug-cc-pVXZ basis sets with X = D, T, Q [10, 11].

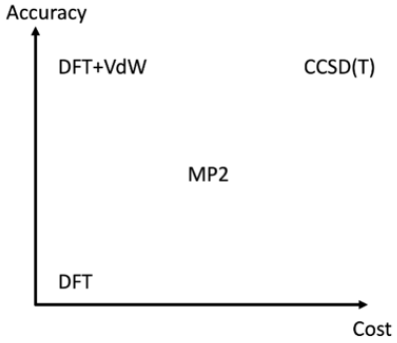

Fig. 2. Scheme of the methods accuracy versus the computational cost to calculate the strength of an hb (considering that the same basis set is used in all the depicted methods).

Conventional and non-conventional HBs

According to the International Union of Pure and Applied Chemistry (IUPAC), to have an hb the D atom should be more electronegative than H [12]. Also, in the IUPAC definition is mentioned that in hydrogen bonded dimers the D-H vibrational frequency is usually red shifted, as compared to that frequency of the isolated monomer [12]. Moreover, in textbooks it is usually mentioned that the A and D atoms tend to be N, O and F. The hbs that follow all these characteristics are classified as conventional, if they do not, thus they are classified as non-conventional. Evidence of non-conventional hbs starts to appear in the literature about the year 2000 when Vargas et al. showed using the MP2/aug-cc-pVTZ level of theory that the strength of -C-H···O contacts is large enough, on the order of 2 to 4 kcal/mol, to be considered as hbs [13]. Our group also showed that non-conventional hbs can be formed when the H atom is more electronegative than the donor one, as in $(HSiN)_2$, $(HGeN)_2$ and $(HSnN)_2$ [11]. However, the $(HNSi)_2$, $(HNGe)_2$ and $(HNSn)_2$ set of dimers, in which the D atom is more electronegative than H, do not form hbs. The formation of a hb was corroborated showing the dependence of the hb strength with respect to the -D-H···A angle, i.e., the hb directionality. Also, it was analyzed the values of the density at the density critical points, the electrostatic potential associated to each dimer, the alteration of the D-H vibrational frequency and the magnitude of the dipole moment as compared against the isolated monomers. The latter study [11] was carried out at the MP2 and CCSD(T) level of theory with the aug-cc-pVXZ basis set family with X = D, T, Q. The formation of hbs when the H atom is more electronegative than the donor one has been corroborated experimental and theoretically in $(CH_3)_3Si\cdots Y$ (Y = ICF3, BrCN, and HCN) by Hobza et al [14]. Thus, it is not necessary for the H atom to be less electronegative than the D one to form an hb. Therefore, it could be considered by the IUPAC to remove the sentence about the H atom electronegativity from the definition of a hb. Another type of non-conventional hb is when π electrons act as the A region. Galano et al. studied such non-conventional hbs between HF, cyclopropane derivatives and ethylene [15,16]. In these cyclopropane derivatives the C-C bonds have an extra p character according to a natural bond orbital analysis. Contrasting the interaction between HF and the ethylene double bond, and those between HF and the C-C bonds in the cyclopropane derivatives, Galano et al. [15] provided evidence of the

J. Mex. Chem. Soc. **2025**, *69*(1)
Special Issue

ISSN-e 2594-0317

formation -D-H···p non-conventional hbs in these systems. This has importance in substrate-receptor interactions of complexes formed by drugs used to treat the acquired immune deficiency syndrome [15]. All these results regarding the formation of non-conventional hbs might also indicate that the nature of the hb is still not well understood.

HBs and peptide structure and stability

A peptide is the product of a dehydration reaction between amino acids. If many amino acids are involved in the reaction the product is a linear (poly)peptide chain that eventually becomes a protein. Hydrogen bonding is crucial to understand the stability, structure, and properties of peptides (short polypeptidic chains) and proteins (long polypeptidic chains with biological activity). For example, the helical and sheet conformations of the protein backbone, named protein secondary structure, were predicted considering the conformations that best favor the formation of hbs. However, these geometric criteria were not supported by energetic studies. In a series of works [17-19] we showed, using DFT and PBE, that the helical conformation of peptides is stabilized by hbs, at 0 K in vacuum, only if hb cooperative effects are considered [17]. Nevertheless, we also showed that such helical conformation is marginally stable at room temperature (in vacuum) [18], and that including TS dispersion corrections the helical conformation is significantly stabilized at 0 K [8] and at temperatures as high as 700 K (in gas phase), which is in concordance with gas-phase experimental results [19]. The stability at 700 K was corroborated performing ab-initio molecular dynamics simulations in gas phase at different temperatures using the PBE functional including and excluding TS dispersion corrections. Still, these results [8,17-19] were not convincing for determining if hbs are the main stabilizing interaction of the helical conformation in aqueous solvent, as one can argue that the extended backbone conformation forms more hbs with the solvent molecules than with itself in the solvated helical conformation. By microsolvating the peptide backbone with water molecules, we found that, at 0 K, the helical conformation is still more stable than the extended conformation using DFT/PBE-TS [20,21]. Hydrogen bonding also affects the dipeptide structure by applying compression along the peptide backbone, which explains why β-sheets in proteins are slightly twisted [22]. Moreover, hbs are crucial for the self-assembly mechanism of dipeptides into their crystal structures as these stabilize the zwitterionic state along possible assembly paths [23]. Furthermore, hbs modulate the elastic response of these systems to mechanical stress, for example, they drive the transformation between different helical conformations upon mechanically stressing the system [24], and originate an unusual stiffness in dipeptide crystals, whose DFT-calculated Young's moduli range between 19.7 and 33.3 GPa [25].

HBs and surface reactivity

Surface O-H groups can be found in oxide and hydroxide materials. In the former, due to the deprotonation of adsorbed species like H_2SO_4 on Zr oxides, and in the latter as part of material composition. In both cases such O-H groups affect decisively the surface reactivity leading to superacidity [26] or the modification of the reactivity of groups containing oxygen [27,28]. For example, recently we have shown [27,28] by means of DFT/PBE-TS calculations and surface models, that the lone pair reactivity of the methoxy group (MeO^-) adsorbed on the surface of layered double hydroxides (LDHs), like MgAl-OH and MgGa-OH, is modified due to its interaction with the surface, which is mediated by the hb formation with surface O-H groups. In this manner we have explained why a specific ratio of Al to Mg in these LDHs has the largest LDH catalytic activity in the cyanoethylation of methanol (MeOH) [27], and why MgGa-OH is a better LDH catalyst for the cyanoethylation of 2-propanol than MgAl-OH, and the opposite for the cyanoethylation of MeOH [28]. Surface and interlaminar hydrogen bonding controls the anion diffusion in such LDH materials [29,30], which could further affect the reactivity as it was found that the adsorption of MeO^- is energetically favored in sites in which a chain of hbs can be formed throughout the bulk of the material, thus involving the position of interlaminar OH^- anions. Moreover, according to the energetics of the adsorption of MeOH and MeO^-, both coexist around

J. Mex. Chem. Soc. **2025**, *69*(1)
Special Issue

ISSN-e 2594-0317

the surface deprotonation site. Therefore, if MeO^- diffuses away from deprotonation sites one may expect that more MeOH will transform into MeO^-, which is the reactive species in the third step of the methanol cyanoethylation reaction. In Ref. 29 and 30 it was shown that low energy barriers to diffuse from one minimum to the neighbor one along the LDHs interlaminar space, are due to the formation of hydrogen bonds between the OH^- anion and interlaminar hydroxyl groups.

HBs and reaction mechanisms and equilibrium

The presence of hbs can stabilize structures connected to an equilibrium state, or to one specific path over another thus determining the reaction mechanism or modifying the reactivity of a chemical system. For example, Cedillo et al. have shown that water clusters can activate the chemical bond on Br_2 by hydrogen bonding with it [31], and Galano et al. reported that the clathrate-hydrate formation is inhibited by antifreeze glycoproteins through the formations of hbs [32]. Also, Galano et al. found that transition states of reactions in gas phase involving the hydroxyl radical and hydroxy ethers are altered due to the formation of hbs, which modify their reactivity [33]. Furthermore, Galano et al. have proposed mechanisms in which hbs play a crucial role to explain experimental kinetic data, thus obtaining good agreement between calculated and experimental results [34-36]. Additionally, Cedillo et al. reported that the presence of intramolecular hbs shift the tautomeric equilibrium towards a particular tautomer, such as in phenacylpyridines, and alter its stability and acidity in solution [37]. Such kind of intramolecular hbs can also significantly change the electrostatic potential of polar molecules [38]. Cedillo et al. also showed that hbs confer different degrees of stability to the different phases of AlOOH under pressure by their symmetrization [39].

Origin of HBs and its cooperative effect

Diverse opinions have been advanced about the nature of hydrogen bonding [see e. g. 40, 41]. The question that one may try to answer is why the interaction energy of the D-H···A is larger than the one expected solely from dispersion forces plus classical dipole-dipole interactions. It has been postulated that the hb strength arises from the sum of different energy contributions like these associated to charge transfer, partial covalency, polarization and electronic resonance [41]. Still, no consensus has been reached about the main contributions to the strength of the hbs. It is well established that two or more hydrogen bonds may interact with each other if they are close enough and aligned, or close to the alignment, provoking a change in their strength. Usually, such interactions among hbs strengthen them, thus this phenomenon is named hb cooperative effect. Little it has been discussed in the literature about the nature of the hb cooperative effect, which may be of different nature than the one of the hb itself. Recently, we have proposed [2] that the hb strength, E_{hb}, in a dimer can be estimated according to

$$E_{hb} = R_{rep} - \frac{2\mu^2}{\lambda^3} \qquad \text{Eq. 1}$$

in which R_{rep} stands for a repulsive contribution, μ for an effective dipole moment (which is different to the molecular dipole moment either in the isolated monomers or in the dimer, see below). λ stands for the distance between the centers of mass of each monomer in the interacting conformation. The second term in right hand side of Eq. 1 is the classical expression for calculating the interaction energy between two point-dipoles aligned head to tail. Recalling that the dipole-dipole interaction energy in a finite chain of *M* dipoles of the same strength aligned head to tail and equally spaced is given by [42]:

J. Mex. Chem. Soc. **2025**, *69*(1)
Special Issue

ISSN-e 2594-0317

$$E_d = \frac{1}{2}\sum_i^M \sum_{j\neq i}^M \frac{-2\mu^2}{\lambda_{ij}^3} = -\frac{2\mu^2}{\lambda^3}\left[\frac{M-1}{1^3} + \frac{M-2}{2^3} + \frac{M-3}{3^3} + \cdots + \frac{1}{(M-1)^3}\right] = -\frac{2\mu^3}{\lambda^3}\sum_i^M \left(\frac{M}{i^3} - \frac{1}{i^2}\right) = -\frac{2\mu^2}{\lambda^3}(M\zeta_3 - \zeta_2) \quad \text{Eq. 2}$$

where ζ_x stands for the Riemann zeta function of order *x* [42]. Dividing Eq. 2 by *M* and taking the limit in which *M* tend to infinity one gets:

$$E_d^\infty = -\frac{2\mu^2}{\lambda^3}\zeta_3 \quad \text{Eq. 3}$$

which is the interaction energy between two point-dipoles embedded in an infinite chain of point-dipoles of the same magnitude, equally spaced and aligned head to tail. Eq. 3 illustrates cooperativity in a point-dipole chain. As for $M \to \infty$ $\zeta_3 \approx 1.2021$, hence the dipole-dipole interaction strengthens by ~1.2021 in an infinite chain owing to the addition of interactions with second, third and so on nearest neighbors. Considering Eq. 3 Nochebuena et al. [2] proposed that the hb strength in an infinite chain, E_{hb}^∞ (see Fig. 1), can be estimated with the next expression:

$$E_{hb}^\infty = R_{rep} - \frac{2\mu^2}{\lambda^3}\zeta_3 \quad \text{Eq. 4}$$

If one hypothesizes that R_{rep} and μ in Eq. 1 and Eq. 4 are the same for a given value of λ, then one is considering that the R_{rep} and μ are readily determined once the first hb is formed. Thus, μ should accounts for all possible quantum effects associated to the attractive energetic contributions to the hb strength, and R_{rep} the repulsive energetic contributions. The R_{rep} term may arise when the electronic cloud around the H atom overlaps with the electronic cloud around the A atom (or region), likely due to the Pauli repulsion. Considering the hypothesis above mentioned, the hb cooperativity can be estimated with the next equation:

$$C_{hb}^\infty = -\frac{2\mu^2}{\lambda^3}(\zeta_3 - 1) \quad \text{Eq. 5}$$

which allows us to argue that hb cooperativity originates solely from dipole-dipole interactions. Eq. 1, 4 and 5 were numerically corroborated by Nochebuena et al. [2] calculating E_{hb} in some hydrogen bonded dimers (hydrogen cyanide, 4-pyridone and formamide dimers), and E_{hb}^∞ in the corresponding infinite chains for different λ values. In all these systems the molecular dipoles are aligned head to tail and the geometry of the molecules in the dimers is the same of the molecules at the infinite chain. DFT/PBE and DFT/PBE0 were used in these calculations together with the TS dispersion correction.

One can argue that equations 1, 4 and 5 are a consequence of the HFT, which estates that

$$\frac{\partial E}{\partial L} = \left\langle \Psi \middle| \frac{\partial \mathcal{H}}{\partial L} \middle| \Psi \right\rangle \quad \text{Eq. 6}$$

where *L* is an arbitrary parameter. Feynman demonstrated that forces acting on nuclei of a molecule can be determined from classical electrostatic calculations once the corresponding electronic charge density is known [43]. For demonstrating that, Feynman used the HFT. In following works other authors used the HFT to demonstrate that the attractive force between two atoms, e.g., two Xe or two Ar atoms, is of the order of $1/R^7$ where R is the distance separating them. These results imply that the appearance of dispersion forces between two charge distributions can be explained with the HFT [44-49], as Feynman mentioned in his seminal work [43]. Thus, in this section we seek for a theoretical support for Eq. 1, 4 and 5 using the HFT.

J. Mex. Chem. Soc. **2025**, *69*(1)
Special Issue

ISSN-e 2594-0317

Let us consider two identical monomers electrically neutral with *N* electrons each capable of forming hbs. The centers of mass of these monomers are located at points p an q along the $\hat{z}$ axis, at opposite sides of the origin o and at a distance $\lambda/2$ from it (Fig. 3). The λ value is such that the monomers are hydrogen bonded. Considering that the Hamiltonian for that system is:

$$\mathcal{H} = -\frac{1}{2}\sum_K \nabla_K^2 - \frac{1}{2}\sum_i \nabla_i^2 + \frac{1}{2}\sum_K \sum_{K' \neq K} \frac{Z_k Z_{K'}}{R_{KK'}} - \sum_K \sum_i \frac{Z_K}{r_{iK}} + \sum_i \sum_{j>i} \frac{1}{r_{ji}^2} \qquad \text{Eq. 7}$$

where the indexes K and K'run over all nuclei in the dimer, Z_K stands for the K-th nuclear charge, $R_{KK'}$ for the distance between the K-th and K'-th nuclei and r_{iK} for the distance between the i-th electron and the K-th nucleus. The $1/2$ factor in the third term of the right-hand side of Eq. 7 stands for compensating double counting. The derivative with respect to λ of the first, second and last terms of the right-hand side of Eq. 7 are zero (these terms do not depend on λ), hence according to the HFT one gets that the energy derivative with respect to λ of the total energy of the resulting dimer is given by:

$$\frac{\partial E_{dim}}{\partial \lambda} = -\frac{1}{2}\sum_K \sum_{K' \neq K} \frac{Z_K Z_{K'}}{R_{KK'}^2} \frac{\partial R_{KK'}}{\partial \lambda} + \sum_K \sum_i Z_K \int \frac{\Psi^*(\vec{r}_1, \cdots, \vec{r}_k, \cdots, \vec{r}_{2N}, \lambda)\Psi(\vec{r}_1, \cdots, \vec{r}_k, \cdots, \vec{r}_{2N}, \lambda)}{r_{iK}^2} \frac{\partial r_{kK}}{\partial \lambda} d\vec{r} \qquad \text{Eq. 8}$$

The λ term in the wavefunction is added just to remark its parametric dependence of such parameter. Integrating the second term of the right-hand side of Eq. 8 over all the electronic coordinates but *i*-th one, one gets:

$$\frac{\partial E_{dim}}{\partial \lambda} = -\frac{1}{2}\sum_K \sum_{K' \neq K} \frac{Z_K Z_{K'}}{R_{KK'}^2} \frac{\partial R_{KK'}}{\partial \lambda} + \sum_K Z_K \int \frac{\rho(\vec{r}, \lambda)}{r_K^2} \frac{\partial r_K}{\partial \lambda} d\vec{r} \qquad \text{Eq. 9}$$

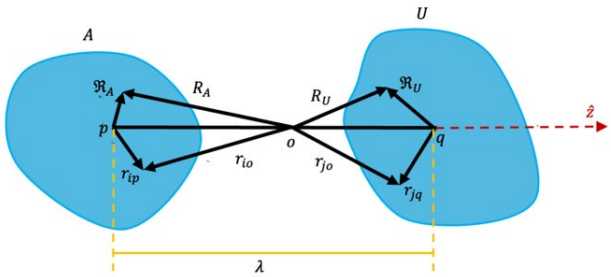

Fig. 3. Scheme for the charge distribution in a hydrogen bonded dimer. The origin of the system is at o, the local origin of the left charge distribution is at p and that for the right charge distribution is at q.

where r_K is the distance between an electron and the K-th nucleus. Recalling that $E_{hb} = E_{dim} - 2E_{mon}$, where E_{dim} is the total energy of the hydrogen bonded dimer and E_{mon} the total energy of the monomer, and assuming that the electron density of the dimer, $\rho(\vec{r}, \lambda)$, can be partitioned we obtain an expression for $\partial E_{hb}/\partial\lambda$. The density of the dimer, $\rho(\vec{r}, \lambda)$, is partitioned according to $\rho(\vec{r}, \lambda) = \rho_p(\vec{r}_p) + \rho_q(\vec{r}_q) + \Delta\rho(\vec{r}, \lambda)$, where $\rho_p(\vec{r}_p)$ and $\rho_q(\vec{r}_q)$ stand for the electron densities of the monomers centered at points p and q (see Figure 3), and $\Delta\rho(\vec{r}, \lambda)$ is a function whose values are such that the density partition expression is exactly fulfilled. To simplify the expression for $\partial E_{hb}/\partial\lambda$ we also assume that the dimer is linear, with their nuclei laying along the z axis. Although Eq. 1, 4 and 5 are also fulfilled even in cases in which not all nuclei lie along the $\hat{z}$ axis, like in the formamide chain [2] and water chains (Rojas-Regalado, S.; Bautista-Renedo, J.; Ireta, J. *in preparation*). Hence, it can be shown that $\partial E_{hb}/\partial\lambda$ becomes

J. Mex. Chem. Soc. **2025**, *69*(1)
Special Issue

ISSN-e 2594-0317

$$\begin{aligned}\frac{\partial E_{hb}}{\partial\lambda} = &-\frac{1}{2}\sum_A\sum_U \frac{Z_A Z_U}{R_{AU}^2}\frac{\partial R_{AU}}{\partial\lambda} \\ &-\frac{1}{2}\sum_U\sum_A \frac{Z_U Z_A}{R_{UA}^2}\frac{\partial R_{UA}}{\partial\lambda} + \frac{1}{2}\sum_K Z_K \int \frac{\rho_p(\vec{r}_p)}{r_{pK}^2}\frac{\partial r_{pK}}{\partial\lambda} d\vec{r}_p \\ &+\frac{1}{2}\sum_K Z_K \int \frac{\rho_q(\vec{r}_q)}{r_{qK}^2}\frac{\partial r_{qK}}{\partial\lambda} d\vec{r}_q \\ &+\frac{1}{2}\sum_K Z_K \int \frac{\Delta\rho(\vec{r}_p,\lambda)}{r_{pK}^2}\frac{\partial r_{pK}}{\partial\lambda} d\vec{r}_p \\ &+\frac{1}{2}\sum_K Z_K \int \frac{\Delta\rho(\vec{r}_q,\lambda)}{r_{qK}^2}\frac{\partial r_{qK}}{\partial\lambda} d\vec{r}_q\end{aligned} \qquad \text{Eq. 10}$$

where the index *A* runs only along nuclei of monomer A (to the left of the origin, Fig. 3) and index *U* runs only along nuclei of monomer U (to the right of the origin, Fig. 3). The 1/2 factor multiplying the integrals on the right-hand side of Eq. 10 arises because we are considering the average of the two ways of calculating $\partial r_K/\partial\lambda$ (i. e. with respect to the origin *p* and with respect to the origin *q*) as it was suggested by Berlin [49]. The negative of the right side of Eq. 10 are the forces exerted on the atoms of the dimer for a given value of λ. Integrating Eq. 10 with respect to λ, and using a Taylor expansion to describe R^{-1} and r^{-1} as an infinite series, and further considering that the monomers are identical one may find that

$$\begin{aligned}E_{hb} = &\sum_A\sum_U Z_A Z_U\left(\frac{\mathcal{R}_{AU}^2}{\lambda^3}+\frac{\mathcal{R}_{AU}^4}{\lambda^5}+\cdots\right) \\ &-\sum_K Z_K\int\rho_p(\vec{r}_p)\left[\frac{(\vec{r}_{pK}\cdot\hat{z})^2}{\lambda^3}+\frac{(\vec{r}_{pK}\cdot\hat{z})^4}{\lambda^5}+\cdots\right]d\vec{r}_p \\ &-\frac{1}{2}\sum_K Z_K\int\Delta\rho(\vec{r}_p,\lambda)\left[\frac{(\vec{r}_{pK}\cdot\hat{z})^2}{\lambda^3}+\frac{(\vec{r}_{pK}\cdot\hat{z})^4}{\lambda^5}+\cdots\right]d\vec{r}_p \\ &-\frac{1}{2}\sum_K Z_K\int\Delta\rho(\vec{r}_q,\lambda)\left[\frac{(\vec{r}_{qK}\cdot\hat{z})^2}{\lambda^3}+\frac{(\vec{r}_{qK}\cdot\hat{z})^4}{\lambda^5}+\cdots\right]d\vec{r}_q\end{aligned} \qquad \text{Eq. 11}$$

where $\mathcal{R}_{AU}$ stands for the distance between the *A*-th and *U*-th atoms, whose positions are referred respect to either the point *p* or the point *q*. Considering that $\mu_{Nz} = \sum_K Z_K\mathcal{R}_K$, $\mu_{ez} = \int z\rho(\vec{r})d\vec{r}$, $\sum_A Z_A = N$, $\rho_p(\vec{r}) = \rho_q(\vec{r})$, and $\int\rho_p(\vec{r})d\vec{r} = N$, Eq. 11 can be rewritten as:

$$\begin{aligned}E_{hb} = &-\frac{2}{\lambda^3}\Big[\mu_{Nz}^2 - \sum_A NZ_A z_A^2 + \mu_{ex}^2 + \frac{1}{2}\int z^2\Delta\rho(\vec{r}_p,\lambda)\rho_p(\vec{r}_p')\,d\vec{r}_p d\vec{r}_p' \\ &+\frac{1}{2}\int z^2\Delta\rho(\vec{r}_q,\lambda)\rho_q(\vec{r}_q')\,d\vec{r}_q d\vec{r}_q'\Big] \\ &+\frac{1}{\lambda^5}\sum_A\sum_U Z_A Z_U\mathcal{R}_{AU}^4 - \frac{1}{\lambda^5}\Big[\int z^4\Delta\rho(\vec{r}_p,\lambda)\rho_p(\vec{r}_p')d\vec{r}_p d\vec{r}_p' \\ &+\int z^4\Delta\rho(\vec{r}_q,\lambda)\rho_q(\vec{r}_q')d\vec{r}_q d\vec{r}_q'\Big]+\cdots\end{aligned} \qquad \text{Eq. 12}$$

J. Mex. Chem. Soc. **2025**, *69*(1)
Special Issue

ISSN-e 2594-0317

where *z* stands for the z-coordinate of the given particle (nucleus or electron) respect to either the point *p* or the point q. Now, considering that the molecular dipole moment of the monomer is $\mu_{mz} = \mu_{Nz} - \mu_{ez}$, one can realize that the part in parenthesis of the first term on the right-hand side of Eq. 11 resembles μ_{mz}^2 plus additional squared dipole-like terms that depends on $\Delta\rho(\vec{r},\lambda)$. Therefore, we replace the part in the parenthesis of this term by $\mu_{ef}^2(\lambda)$, the square of a kind of effective dipole. Thus Eq. 12 can be written as

$$E_{hb} = -\frac{2\mu_{ef}^2(\lambda)}{\lambda^3} + \vartheta_{rep}^5 - \vartheta_{att}^5 + \cdots \qquad \text{Eq. 13}$$

where ϑ_{rep}^5 and ϑ_{att}^5 stands for the repulsive and attractive terms that depend on $1/\lambda^5$. Hence, Eq. 13 shows that the leading attractive term contributing to the hb energy can be obtained considering interactions between effective dipoles. Next, if one generates an infinite chain replicating the dimer along a given direction (see Fig. 1), without optimizing the geometry of the resulting chain and ensuring that monomers keep their nearest neighbor distance equal to that in the dimer along the chain, one can find that Eq. 13 can be transformed into

$$E_{hb}^{\infty} = -\frac{2\mu_{ef}^2}{\lambda^3}\zeta_3 + \vartheta_{rep}^5\zeta_5 - \vartheta_{att}^5\zeta_5 + \cdots \qquad \text{Eq. 14}$$

where ζ_5 is the Riemann zeta function of order 5 ($\zeta_5 = 1.037\ldots$). To get Eq. 14 we have applied the same method as for obtaining Eq. 3. Subtracting Eq. 13 from Eq. 14 one arrives to

$$C_{hb}^{\infty} = -\frac{2\mu_{ef}^2}{\lambda^3}(\zeta_3 - 1) + \left(\vartheta_{rep}^5 - \vartheta_{att}^5\right)(\zeta_5 - 1) + \cdots \qquad \text{Eq. 15}$$

Thus, according to Eq. 15 one can argue that the contributions of the second term and higher orders to C_{hb}^{∞} are negligible, hence it is recovered Eq. 5. The only assumption for obtaining Eq. 15 from Eq. 14 is that $\Delta\rho(\vec{r},\lambda)$ is completely determined by first nearest neighbors. Based on PBE-TS and PBE0-TS DFT calculations it was corroborated that such assumption is fulfilled by the systems investigated by Nochebuena et al. [2] and by one dimensional water chains (work in progress -Rojas-Regalado, S.; Bautista-Renedo, J.; Ireta, J. *in preparation*-). In the work of Nochebuena et al. it was proposed an empirical formula for determining μ_{ef} solely knowing the hb in the dimer. Then, with such μ_{ef} it was estimated the hb in the infinite chain within an error of ~0.2 kcal/mol, with respect to the PBE-TS and PBE0-TS DFT results, along all the dissociation path of the chain.

Conclusions

The contributions of the chemical department, at UAM campus Iztapalapa, to advance our understanding of hydrogen bonding has been significative. These contributions have been devoted to investigating the effect of hbs into the physicochemical properties of the systems and to further our understanding of the nature of such interactions. For example, by means of the HFT here it is obtained an expression for the hb strength in a dimer and in an infinite chain. Using these expressions, it is corroborated that the hb cooperativity arises solely from the classical interaction among effective point dipoles. Currently, the line of investigation on non-covalent interaction is still vigorous at the theoretical physical chemistry area of the chemistry department at UAM, campus Iztapalapa. We aim for getting a concise theory on non-covalent interactions.

Acknowledgements

We wish to acknowledge funding from CONAHCYT, projects A1-S-42775 and 1561802. B. G. acknowledges CONAHCYT for a postdoctoral fellowship through the project 1561802.

J. Mex. Chem. Soc. **2025**, *69*(1)
Special Issue

ISSN-e 2594-0317

References

1. Latimer, W. M.; Rodebush, W. H. *J. Am. Chem. Soc.* **1920**, *42*, 1419-1433. DOI: https://doi.org/10.1021/ja01452a015.
2. Nochebuena, J.; Cuautli, C.; Ireta, J. *Phys. Chem. Chem. Phys.* **2017**, *19*, 15256-15263. DOI: https://doi.org/10.1039/C7CP01695F.
3. Pittner, J.; Hobza, P. *Chem. Phys. Lett.* **2004**, *390*, 496-499. DOI: https://doi.org/10.1016/j.cplett.2004.04.009.
4. Cremer, D. *WIREs Comput. Mol. Sci.* **2011**, *1*, 509–530. DOI: https://doi.org/10.1002/wcms.58.
5. Vargas, R.; Garza, J.; Friesner, R. A.; Stern, H.; Hay, B. P.; Dixon, D. A. *J. Phys. Chem. A.* **2001**, *105*, 4963–4968. DOI: https://doi.org/10.1021/jp003888m.
6. Perdew, J. P.; Burke, K.; Ernzerhof M. *Phys. Rev. Lett.* **1996**, *77*, 3865-3868. DOI: https://doi.org/10.1103/PhysRevLett.77.3865.
7. Ireta, J.; Neugebauer, J.; Scheffler, M. *J. Phys. Chem. A.* **2004**, *108,* 5692-5698. DOI: https://doi.org/10.1021/jp0377073.
8. Nochebuena, J.; Ramírez, A.; Ireta, J. *Int. J. Quantum Chem.* **2015**, *115*, 1613-1620. DOI: https://doi.org/10.1002/qua.24993.
9. Tkatchenko, A.; Scheffler, M. *Phys. Rev. Lett.* **2009**, *102*, 073005. DOI: https://doi.org/10.1103/PhysRevLett.102.073005.
10. Bautista-Renedo, J.; Ireta, J. *Phys. Chem. Chem. Phys.* **2024**, *26*, 21468-21475. DOI: https://doi.org/10.1039/D4CP00907J.
11. Bautista-Renedo, J.; Reyes-Pérez, H.; Cuevas-Yáñez, E.; Barrera-Díaz, C.; González-Rivas, N.; Ireta, J. *RSC Adv.* **2019**, *9*, 5937-5941. DOI: https://doi.org/10.1039/C9RA00856J.
12. Arunan, E.; Desiraju, G. R.; Klein, R. A.; Sadlej, J.; Scheiner, S.; Alkorta, I.; Clary, D. C.; Crabtree, R. H.; Dannenberg, J. J.; Hobza, P.; Kjaergaard, H. G.; Legon, A. C.; Mennucci, B.; Nesbitt, D. *J. Pure Appl. Chem.* **2011**, *83*, 1637–1641. DOI: https://doi.org/10.1351/PAC-REC-10-01-02.
13. Vargas, R.; Garza, J.; Dixon, D. A.; Hay, B. P. *J. Am. Chem. Soc.* **2000**, *122*, 4750-4755. DOI: https://doi.org/10.1021/ja993600a.
14. Civiš, S.; Lamanec, M.; Špirko, V.; Kubišta, J.; Špet´ko, M.; Hobza, P. *J. Am. Chem. Soc.* **2023**, *145*, 8550-8559. DOI: https://doi.org/10.1021/jacs.3c00802.
15. Galano, A.; Alvarez-Idaboy, J. R.; Vivier-Bunge, A.; *Theor. Chem. Acc.* **2007**, *118*, 597-606. DOI: https://doi.org/10.1007/s00214-007-0353-z.
16. Galano, A.; Narciso-Lopez, M.; Francisco-Marquez, M. *J. Phys. Chem. A.* **2010**, *114*, 5796-5809. DOI: https://doi.org/10.1021/jp101157b.
17. Ireta, J.; Neugebauer, J.; Scheffler, M.; Rojo, A.; Galván, M.; *J. Phys. Chem. B*. **2003**, *107*, 1432-1437. DOI: https://doi.org/10.1021/jp026848m.
18. Ismer, L.; Ireta, J.; Neugebauer, J. *J. Phys. Chem. B*. **2008**, *112*, 4109-4112. DOI: https://doi.org/10.1021/jp077728n.
19. Tkatchenko, A., Rossi, M.; Blum, V.; Ireta, J.; Scheffler, M. *Phys. Rev. Lett.* **2011**, *106*, 118102. DOI: https://doi.org/10.1103/PhysRevLett.106.118102.
20. Ireta, J. *Theor. Chem. Acc.* **2016**, *135*, 220. DOI: https://doi.org/10.1007/s00214-016-1981-y.
21. Ireta, J. Int. *J. Quantum Chem* **2012**, *112*, 3612-3617. DOI: https://doi.org/10.1002/qua.24246.
22. Ireta, J. *J. Chem. Theory Comput.* **2011**, *7*, 2630-2637. DOI: https://doi.org/10.1021/ct2002144.
23. González-Díaz, N. E.; López-Rendón, R.; Ireta, J. *J. Phys. Chem. C.* **2019**, *123*, 2526−2532. DOI: https://doi.org/10.1021/acs.jpcc.8b10340.
24. Ireta, J.; Neugebauer, J.; Scheffler, M.; Rojo, A.; Galván, M. *J. Am. Chem. Soc.* **2005**, 1*27*, 17241-17244. DOI: https://doi.org/10.1021/ja053538j.
25. del Campo, J. M.; Ireta, J. *Phys. Chem. Chem. Phys.* **2021**, *23*, 11931-11936. DOI: https://doi.org/10.1039/d0cp06018f.
26. Ireta, J.; Aparicio, F.; Viniegra, M.; Galván, M. *J. Phys. Chem. B.* **2003**, *107*, 811-818 DOI: https://doi.org/10.1021/jp026852v.

J. Mex. Chem. Soc. **2025**, *69*(1)
Special Issue

ISSN-e 2594-0317

27. Cuautli, C.; Valente, J. S.; Conesa, J. C.; Ganduglia-Pirovano, M. V.; Ireta, J. *J. Phys. Chem. C*. **2019**, *123*, 8777−8784. DOI: https://doi.org/10.1021/acs.jpcc.8b10935.
28. Castro, G.; Valente, J. S.; Galván, M.; Ireta, J. *Phys. Chem. Chem. Phys.* **2022**, *24*, 23507-23516. DOI: https://doi.org/10.1039/d2cp02704f.
29. Cuautli, C.; Ireta, J. *J. Chem. Phys.* **2015**, *142*, 094704. DOI: https://doi.org/10.1063/1.4913570.
30. Nieto-Malagón, G.; Cuautli, C.; Ireta, J. *J. Phys. Chem. C*. **2018**, *122*, 171−176. DOI: https://doi.org/10.1021/acs.jpcc.7b10384.
31. Santoyo-Flores, J. J.; Cedillo, A.; Bernal-Uruchurtu, M. I. *Theor. Chem. Acc.* **2013**, *132*, 1-7. DOI: https://doi.org/10.1007/s00214-012-1313-9.
32. Cruz-Torres, A.; Romero-Martínez, A.; Galano, A. *Chem. Phys. Chem.* **2008**, *9*, 1630-1635. DOI: https://doi.org/10.1002/cphc.200800241.
33. Galano, A.; Alvarez-Idaboy, J. R.; Ruiz-Santoyo, M. A.; Vivier-Bunge, A. *Chem. Phys. Chem.* **2004**, *5*,1379-1388. DOI: https://doi.org/10.1002/cphc.200400127.
34. Galano, A.; Alvarez-Idaboy, J. R.; Ruiz-Santoyo, M. E.; Vivier-Bunge, A. *J. Phys. Chem. A*. **2005**, *109*, 169-180. DOI: https://doi.org/10.1021/jp047490s.
35. Galano, A.; Alvarez-Idaboy, J. R.; Ruiz-Santoyo, M. A.; Vivier Bunge, A. *Chem. Phys. Chem.* **2004**, *5*, 1379-1388. DOI: https://doi.org/10.1002/cphc.200400127.
36. Zavala-Oseguera, C.; Alvarez-Idaboy, J. R.; Merino, G.; Galano, A. *J. Phys. Chem. A*. **2009**, *113*, 13913-13920. DOI: https://doi.org/10.1021/jp906144d.
37. Cedillo, A.; Kvedaravičiūtė, S.; Aidas, K. *Theor. Chem. Acc.* **2020**, *139*, 52. DOI: https://doi.org/10.1007/s00214-020-2558-3.
38. González-Rivas, N.; Cedillo, A. *Comput. Theor. Chem.* **2012**, *994*, 47-53. DOI: https://doi.org/10.1016/j.comptc.2012.06.012.
39. Cedillo, A.; Torrent, M.; Cortona, P. *J. Phys.: Condens. Matter*. **2016**, *28*, 185401. DOI: https://doi.org/10.1088/0953-8984/28/18/185401.
40. Clark, T.; Murray, J. S.; Politzer, P. *Phys. Chem. Chem. Phys.* **2018**, *20*, 30076-30082. DOI: https://doi.org/10.1039/C8CP06786D.
41. van der Lubbe, S. C. C.; Fonseca Gerra, C. *Chem. Asian J.* **2019**, *14*, 2760-2769. DOI: https://doi.org/10.1002/asia.201900717.
42. Allen, P. B. *J. Chem. Phys.* **2004**, *120*, 2951-2962. DOI: https://doi.org/10.1063/1.1630029.
43. Feynman, R. P. *Phys. Rev.* **1939**, *56*, 340-343. DOI: https://doi.org/10.1103/PhysRev.56.340.
44. Salem, L.; Wilson, E. B. Jr. *J. Chem. Phys.* **1962**, 36, 3421-3427. DOI: https://doi.org/10.1063/1.1732475.
45. Hirschfelder, J. O.; Eliason, M. A. *J. Chem. Phys.* **1967**, *47*, 1164-1169. DOI: https://doi.org/10.1063/1.1712002.
46. Bader, R. F. W.; Chandra, A. K. *Can. J. Chem*. **1968**, *46*, 953-966. DOI: https://doi.org/10.1139/v68-157.
47. Hunt, K. L. C. *J. Chem. Phys.* **1990**, *92*, 1180-1187 DOI: https://doi.org/10.1063/1.458126.
48. Politzer, P.; Murray, J. S. *J. Mol. Model.* **2018**, *24*, 266. DOI: https://doi.org/10.1007/s00894-018-3784-7.
49. Berlin, T. *J. Chem. Phys.* **1951**, *19*, 208-213. DOI: https://doi.org/10.1063/1.1748161.